BOX fMRI using Multiple-Acquisition Steady-State Free Precession Imaging for Full-Brain Coverage

J. Lee[1], P. T. Gurney[1], S. O. Dumoulin[2], B. A. Wandell[2], A. Shankaranarayanan[3], D. G. Nishimura[1], J. M. Pauly[1]

[1]Electrical Engineering, Stanford University, Stanford, CA, United States, [2]Psychology, Stanford University, Stanford, CA, United States, [3]Global Applied Science Laboratory, GE Healthcare, Menlo Park, CA, United States

Introduction A new fMRI method, which we refer to as BOX (Blood OXygenation), generates oxygenation level dependent contrast using the T_2 sensitive steady state of SSFP imaging. BOX has large coverage over the off-resonance frequency range because SSFP imaging is sensitive to T_2 changes over a broad range of off-resonance frequencies [1]. Large off-resonance creates mere banding as opposed to GRE acquisitions used for BOLD where severe signal dropout and image distortions occur in areas with large off-resonance gradients. The banding can be easily removed with two acquisitions [2]. By using two acquisitions, distortion-free high spatio-temporal resolution 3D full-brain coverage can be obtained.

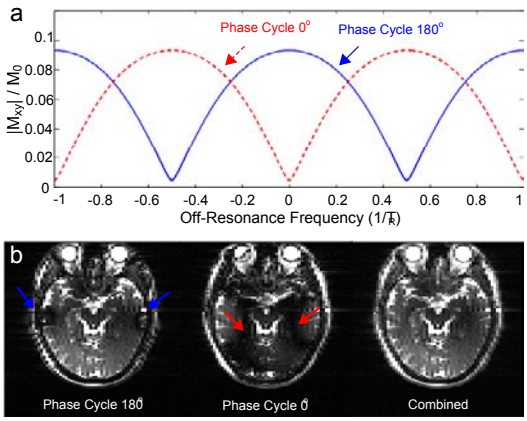

Figure 1 Multiple-acquisition scheme for BOX. (a) SSFP imaging results in periodic banding with increasing off-resonance frequency which can be manipulated by changing the phase-cycling angle. (b) 3DFT SSFP images with 180° and 0° phase cycling and the combined image (MIP).

Theory Off-resonance observed within a brain usually exceeds a single-band of an off-resonance profile (determined by T_R), which leads to banding. This problem can be easily solved using two acquisitions. By acquiring one set of data with a 180° phase cycling and another with 0° phase cycling, the image essentially becomes free of regions with no signal (banding) (Fig. 1). This allows the full-brain coverage including areas of large off-resonance gradients (e.g. air-tissue boundary).

The two sets of data can then be combined using different approaches including maximal intensity projection (MIP). For the combination of the fMRI data sets, temporal averages of the two data sets were first calculated. From the two temporal averages, masks were created to indicate the regions in which each average data set has higher signal intensity. For the functional analysis, a combined data set was created by applying the previously calculated mask to each data set. For voxels where the first data set average had a higher signal intensity, the values from the first image will be selected and vice versa.

Methods To demonstrate the whole brain imaging capability of this method, an fMRI experiment that generates a broad area of activation was used. The experiment involved a line drawing recognition task which is known to activate the visual area, the language processing area and the memory region. The stimulus (Fig. 2) consisted of line drawings that are on and off for 15 s at a time. During the "on" period, a line drawing appears for 1 s at a time, 12 times during the 15 s. Each time an image appears, the subject was instructed to think of the name of the object.

The experiments were conducted on a GE 3 T EXCITE whole-body scanner with a maximum gradient amplitude of 40 mT/m and maximum slew rate of 150 mT/m/ms. The BOX imaging was performed with a FOV of 24 x 24 x 4 cm^3 and a 2 mm isotropic resolution using 3D stack-of-spiral acquisitions [3]. T_R was 7.8 ms while minimum T_E (0.64 ms) was chosen. The resulting temporal resolution was 2.5 s per volume with 48 temporal frames acquisitions over 2 min. BOLD images were also acquired for comparison. The BOLD imaging protocol was designed to have the same temporal resolution as the BOX experiment. Multi-slice single-shot EPI imaging was performed with T_R / T_E = 2500 / 50 ms. The FOV was 24 x 24 cm^2 and the resolution was 2 x 2 mm^2. Fifteen 3 mm-thick slices were acquired to yield a 4.5 cm FOV in the slab direction.

Figure 3 fMRI Stimuli.

The BOX and BOLD data was then analyzed using FEAT [4] including motion correction, temporal and spatial filtering (5 mm) and correlation analysis with the standard model for the hemodynamic response to the block stimulus. Activation masks were generated with a Z threshold of 2.3 and cluster threshold of $p < 0.05$.

Results The activation pattern generally shows good agreement for both BOLD and BOX imaging (Fig 3), while BOX activation is more localized to gray matter [5,6]. In the areas with large off-resonance, BOLD images (Fig. 3a) show significant image distortion and signal dropout. The BOX images (Fig. 3b) exhibit mere banding in the areas of large off-resonance. This allows activations near large off-resonance to be reliably detected. The banding artifacts can be eliminated using two acquisitions as shown in Fig. 3c. The BOX images show activations in the area near the sinus which cannot be reliably detected using BOLD. The blue and green circles show activations in the memory and language related area. The activations in the green circle area have only been previously detected using PET (Positron Emission Tomography) imaging.

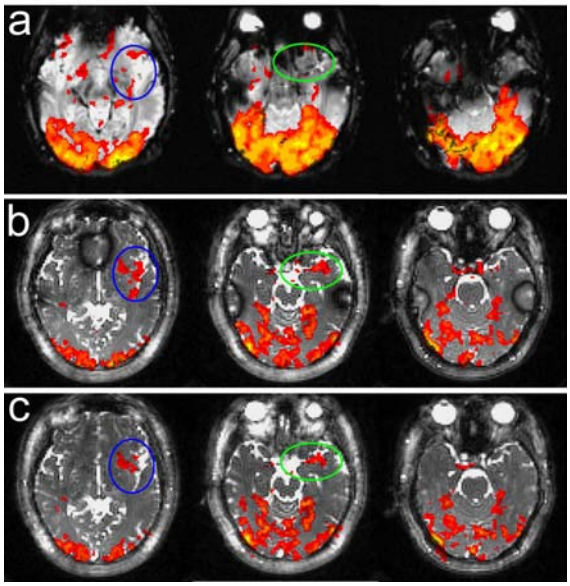

Figure 2 BOLD / BOX comparison on full-brain coverage. (a) The BOLD image shows large activation in a wide area but the activation pattern looks less selective and bulky. (b) The single-acquisition BOX method shows reliable activation throughout the full-brain including the areas with signal loss in BOLD. (c) Two-acquisition BOX further improves the image by completely eliminating regions with low signal (banding regions). The areas with the blue and green circles show activation in the memory and language processing area.

Discussion In regions with high off-resonance gradients, signal dropouts make it impossible to detect any brain activations using BOLD. BOX methods result only in banding artifacts, which can be removed by combining two acquisitions. Thus, the full brain can be monitored for activation in areas that are not accessible with BOLD. Future studies would include experiments designed to activate such regions and comparisons with other neuroimaging modalities such as PET.

References

1. R. Dharmakumar, et al., MRM, 53(3):574–583, 2005.
2. N. K. Bangerter et al., MRM, 51(5):1038–1047, 2004.
3. J. H. Lee et al., MRM, 50(6):1276–1285, 2003.
4. S. M. Smith et al., NeuroImage, 23:S208–S219, 2004.
5. J. L. Boxerman et al., MRM, 34:4–10, 1995.
6. C.V. Bowen et al., In Proc 13th ISMRM, page 119, Miami, 2005.